No time for surface charge: how bulk conductivity hides charge patterns from KPFM in contact-electrified surfaces

Felix Pertl,[1,*] Isaac C.D. Lenton,[1] Tobias Cramer,[2] and Scott Waitukaitis[1]

[1] *Institute of Science and Technology Austria, Am Campus 1, 3400 Klosterneuburg, Austria*
[2] *Department of Physics and Astronomy University of Bologna, Viale Berti Pichat 6/2, 40127 Bologna, Italy*

(Dated: August 13, 2025)

SAMPLE PREPARATION AND CHARACTERIZATION

PDMS samples: As the conducting substrate for a main sample, we used used a gold coated Si-wafer cut it into a square of 1 cm side length. We prepared PDMS by mixing Sylgard™ 184 elastomer base and curing agent in a 10:1 weight ratio. After thoroughly blending with a centrifugal, bubble-free mixer (Hauschild SpeedMixer DAC 150.1, two minutes at 2000 rpm), we spin coated the uncured liquid at 1000 rpm for 1 min onto the gold surface. Baking this in the oven at 80°C for 24 hours resulted in our 'main' PDMS sample with a typical thickness of ∼100 µm. This method was used for all data discussed in the main text.

In Suppl. Fig. 1, we present additional data ('PDMS 65°C') prepared identically, but cured at 65°C instead.

SU-8 samples: We spin-coated SU-8 (GM1075, Gersteltec) onto a gold-coated silicon wafer at 1000 rpm for 1 minute. This was subsequently baked on a hot plate at 150°C for 10 minutes. Typical sample thickness were ∼100 µm.

Mica samples: We used a Mica disk (Agar Scientific) and cleaved it with a razor blade until we reached a thin flat sheet. Typical sample thickness were ∼50 µm.

Polyacrylonitrile samples: Polyacrylonitrile (PAN) was deposited onto a gold wafer with an RF sputtering system (DST3-T, VacTechniche) under argon flow for several hours. Typical sample thicknesses were tens of nanometers.

SiO_2 samples: The SiO_2 wafer was obtained from a commercial distributor with a thickness of 3 µm.

PDMS counter samples: When making main PDMS samples, remaining uncured elastomer was poured into a plastic dish, degassed until no bubbles remained and baked for 24 hours at 80°C. From this slab, we cut out counter-samples of PDMS with 1 cm side length, using a custom-fabricated stencil to precisely guide the blade of a clean, fine razor. We adhered each PDMS counter sample to a 3D-printed holder using additional PDMS and further curing at 80°C for 24 hours. Typical counter samples had a thickness of a few millimeters. We used the 'air-facing' side of these samples for contact.

We used a second method to make PDMS counter samples following Ref. [1]. Instead of curing the PDMS in a plastic dish, we cast it onto a silanized Si-wafer (1H, 1H, 2H, 2H-perfluorooctyltrichlorosilane) and baked it at 65°C for 24 hours. We gently peeled off the PDMS from the wafer and cut it into squares. These were rinsed with dichloromethane (DCM) and isopropyl alcohol (IPA) and dried with nitrogen to remove any residue of the silane. We adhered each sample to a 3D-printed holder using additional PDMS, and then let this cure at room temperature for at least 48 hours. We used the 'wafer-facing' side of these samples for contact.

Sample thickness measurements: The thicknesses of PAN and SiO_2 samples were measured with an ellipsometer (Multi-Wavelength, Film-Sense). All other samples were measured using the AFM by bringing the cantilever into contact with the sample on the sample stage, then subtracting the z-scanner position, as detailed in Suppl. Table 1.

Sample discharge: We used a custom-built discharge chamber to remove residual charge from the sample before contact. The chamber housed a photoionizer (Hamamatsu L12645, 10 keV) positioned in front of a fan. Samples were placed downstream in the airflow generated by the fan. As the photoionizer ionized the air, the resulting charged species were carried toward the sample. The sample discharged as its electric field attracted oppositely charged ions.

CHARGE DECAY WITH A VARIETY OF MATERIALS

Here we present further data for a variety of materials with different nominal conductivities. Table 1 shows the relevant parameters for all samples used. Note that, as discussed in the main text, the non-Ohmic nature of the materials leads to nominal values for conductivity that can vary over several orders of magnitude for a given material (last two columns in table).

Suppl. Fig. 1 shows measured KPFM potentials for each material after contact, unfolded from the space domain to the time domain. All data is normalized to the initial measured potential for visual aid. For the 'best' insulator

SUPPL. TABLE 1. Properties of materials used: thickness d, permittivity κ and bulk conductivity c; †provided by distributor.

Material	d (μm)	κ_{max}	κ_{min}	c_{max} (S/m)	c_{min} (S/m)
SU-8	∼200	4.1[2]	2.85 [3]	5×10^{-16}[4]	1.28×10^{-13}[5]
PDMS 65°C	∼100	3.0[6]	2.55[6]	2.5×10^{-14}[7]	10^{-12}[8]
PDMS 80°C	∼100	3.0[6]	2.55[6]	2.5×10^{-14}[7]	10^{-12}[8]
Mica	∼57	9.3[9]	6.4[9]	5×10^{-16}†	2.5×10^{-13}†
PAN	0.021	4.2[7]	2.87[7]	10^{-15}[10]	10^{-11}[7]
SiO_2	3†	3.9[11]	3.7[11]	10^{-16}[12]	10^{-13} [13]

(SiO_2), the decay appears linear over the timescale shown; over longer timescales its decay slows down. As the nominal conductivities increase, the decays clearly occur more quickly, with the fastest corresponding to the 'worst' insulator, PDMS.

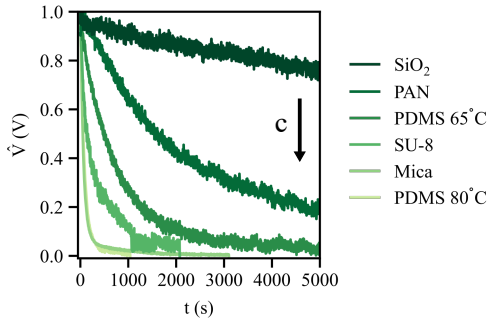

SUPPL. FIG. 1. Better insulators decay more slowly. When we unfold spatial KPFM data into the time domain for many materials of varying conductivities, we see that the 'best' insulators (*e.g.* SiO_2) decay slowly, while the 'worst' ones (*e.g.* PDMS) decay quickly. Potentials are normalized to initial values aid visualization.

COLE-COLE RESPONSE FUNCTION AND FIT PARAMETERS

As we explained in the main text, the measured potential decays are not strictly exponential; this is highlighted by plotting them on log-lin scale, as in Suppl. Fig. 2. Ref. [14] developed a more rigorous approach to model such decay considering as a circuit composed of several series cells, each corresponding to an elementary relaxation process. In this framework, a "cell" corresponds to a discrete relaxation mode within the material, capturing contributions from different polarization or charge transport mechanisms. The resulting expression found in that paper is,

$$V(t) = V_0 - \sum_{i=1}^{2} \Delta V_i [1 - E_{\alpha_i}(-(t/\tau_i)^{\alpha_i})] \tag{S1}$$

with α_i, τ_i, ΔV_i and E_{α_i} being characteristic exponent, relaxation time, voltage change and Mittag-Leffler function associated with the i^{th} cell, respectively. Following Ref. [14] two cells are sufficient to fit the relaxation dynamics in our data. We use Eq. S1 to fit the experimental data (green dots) and find good agreement, as shown by the black dashed line in Suppl. Fig. 2.

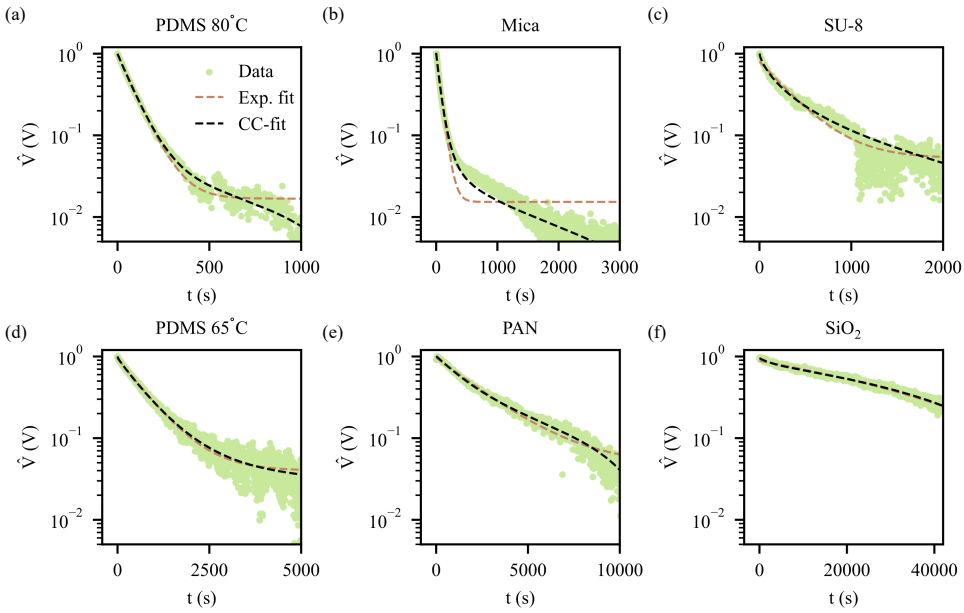

SUPPL. FIG. 2. Comparison between exponential fit and Mittag-Leffler fit. (a)-(f) We compare the exponential model (Exp. fit) and the response function model (CC-fit) for all used materials on log-lin plots. Normalized potentials are shown for visual aid. In all cases, Cole-Cole response model fits as well or better. Fit values are listed in Suppl. Tables 2 and 3, respectively.

SUPPL. TABLE 2. Fit parameters used for the exponential function: initial potential V_0, characteristic time constant τ and the back ground potential V_{bg}

Material	V_0 (V)	τ (s)	V_{bg} (V)
SU-8	0.75	337	0.05
PDMS 65°C	0.9	740	0.04
PDMS 80°C	0.96	86	0.02
Mica	1.0	70	0.02
PAN	0.92	2482	0.05
SiO_2	1.35	65105	-0.46

SUPPL. TABLE 3. Fit parameters used for the Cole-Cole response function: initial potential V_0, potential decay contribution of corresponding cell ΔV, characteristic time constant τ and characteristic exponent α

Material	V_0 (V)	ΔV_1 (V)	ΔV_2 (V)	τ_1 (s)	τ_2 (s)	α_1	α_2
SU-8	1.0	1.05	0	255	4591	0.73	0.31
PDMS 65°C	1.0	0.1	0.9	441	720	0.36	0.97
PDMS 80°C	1.0	0.97	0.15	81	5672	0.98	1.0
Mica	1.02	0.99	0.07	64	4736	0.94	0.45
PAN	1.01	0.73	1.59	1612	62035	1.0	1.0
SiO_2	0.95	0.13	2.54	2639	163213	0.96	1.0

ADDITIONAL PLOTS RELEVANT TO THE MAIN TEXT

Before each contact experiment, we measure the KPFM potential in a fully discharged state. The potential is smooth and uniform prior to contact, with a mean value of (-0.26 ± 0.05) V for SU-8 and (-0.41 ± 0.03) V for SiO_2, as shown in Suppl. Fig. 3 a and b, respectively.

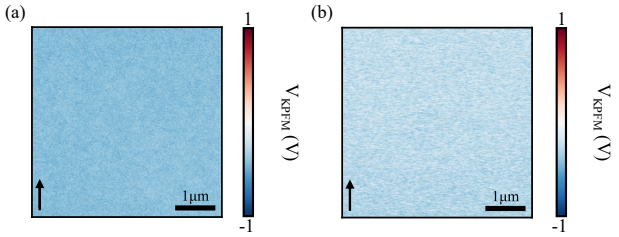

SUPPL. FIG. 3. KPFM scans of Figure 4 prior contact. (a) and (b) show the KPFM scans prior to contact for Figure 4 (a) and (b), respectively. Both exhibit a smooth uniform charge distribution, and both exhibit values that are *different* than immediately after contact, as expected due to the addition of CE-transferred charge.

* felix.pertl@ist.ac.at

[1] H. T. Baytekin, A. Z. Patashinski, M. Branicki, B. Baytekin, S. Soh, and B. A. Grzybowski, Science **333**, 308 (2011).
[2] K. A. Materials, SU-8 2000 datasheet, `https://kayakuam.com/products/display-dielectric-layers/` (2025), accessed: 27 January 2025.
[3] A. Ghannam, C. Viallon, D. Bourrier, and T. Parra, in *2009 European Microwave Conference (EuMC)* (IEEE, 2009) pp. 1041–1044.
[4] M. Tijero, G. Gabriel, J. Caro, A. Altuna, R. Hernández, R. Villa, J. Berganzo, F. Blanco, R. Salido, and L. Fernández, Biosensors and Bioelectronics **24**, 2410 (2009).
[5] Kayaku Advanced Materials, SU-8 3000 datasheet, `https://kayakuam.com/products/su-8-3000/` (2025), accessed: 27 January 2025.
[6] P.-Y. Cresson, Y. Orlic, J.-F. Legier, E. Paleczny, L. Dubois, N. Tiercelin, P. Coquet, P. Pernod, and T. Lasri, IEEE Microwave and Wireless Components Letters **24**, 278 (2014).
[7] W. M. Haynes, D. R. Lide, and T. J. Bruno, *CRC handbook of chemistry and physics*, Vol. 97 (CRC press, 2016) p. 2198.
[8] W. Xu, M. Kranz, S. Kim, and M. Allen, Journal of Micromechanics and Microengineering **20**, 104003 (2010).
[9] J. Weeks Jr, Physical Review **19**, 319 (1922).
[10] I. A. Parinov, S.-H. Chang, and V. Y. Topolov, *Advanced materials: manufacturing, physics, mechanics and applications*, Vol. 175 (Springer, 2015).
[11] B. El-Kareh and L. N. Hutter, *Fundamentals of semiconductor processing technology* (Springer Science & Business Media, 2012).
[12] J. F. Shackelford and W. Alexander, *CRC materials science and engineering handbook* (CRC press, 2000).
[13] F. Palumbo, C. Wen, S. Lombardo, S. Pazos, F. Aguirre, M. Eizenberg, F. Hui, and M. Lanza, Advanced Functional Materials **30**, 1900657 (2020).
[14] P. Molinié, Journal of Applied Physics **134** (2023).